Supporting Information

Layered Sodium Titanate with Matched Lattice: Single Ion Conductor in Solid-State Sodium Metal Battery

Xuanao Ma†, Yang Liu†, Yunhuai Zhang and Yun Gong*

Department of Applied Chemistry, College of Chemistry and Chemical Engineering, Chongqing University, Chongqing 401331, P. R. China. E-mail: gongyun7211@cqu.edu.cn; Tel: +86-023-65678932

S1. Experiment section

S1.1 Synthesis of hydrated NTO

Hydrated NTO was synthesized according to the procedure reported in the literature with some modifications.[1] Firstly, 1.0 mL of tetrabutyl titanate was dissolved into 6.0 mL of *n*-butanol with the stirring via a magnetic stirrer. Then 0.5 mL NaOH aqueous solution (10 M) was added dropwise into the solution, and the reaction mixture was stirred at room temperature for 6 h until the solution became pale-yellow and turbid. Subsequently, the mixture was transferred to a 10 mL Teflon-lined stainless steel autoclave and heated in an oven at 180 ℃ for 12 h. After cooling to room temperature, the obtained white precipitate was washed with distilled water and ethanol for three times. After dried at 60 ℃ overnight, hydrated NTO was obtained.

S1.2 Synthesis of NTO

Hydrated NTO was put in a quartz tubular furnace and sintered at 200 °C for 2 h with a heating rate of 5 °C min^{-1} in N_2 atmosphere, followed by a natural cooling process, then NTO was obtained.

S1.3 Synthesis of NTO microsheets

NTO microsheets can be obtained by recrystallizing NTO in N, N' -dimethylformamide (DMF) or N-methyl-2-pyrrolidone (NMP). A typical procedure is as follows: 30 mg NTO was immersed in 3 mL of the above solvent under sonication, then left to stand for 12 h. Finally, the recrystallized sample was collect via centrifugation and dried in an oven at 60 °C overnight.

S1.4 Fabrication of NTO, NTO CPE and blank SSE

A certain amount of NTO microsheets were cold-pressed into a tablet with a diameter of 10 mm under a pressure of 10 MPa for 5 min, then the obtained tablet (thickness: 200 ~400 μm) was dried in a vacuum at 100 °C for 12 h to obtain NTO inorganic solid-state electrolyte (denoted as NTO).

NTO CPE was prepared based on PVDF-HFP, $NaPF_6$, NTO and DMF in a weight ratio of 30: 6: 14: 50. Firstly, PVDF-HFP (Mw: 400000, Shanghai Macklin Co.) was dissolved in DMF, then $NaPF_6$ was dissolved into the DMF solution. Thirdly, NTO was added into the above solution, and the mixture was vigorously stirred for ~ 24 h until a white homogeneous slurry was obtained. Afterwards, the PVDF-HFP/NTO /$NaPF_6$ slurry was spread on a clean glass plate and dried in an oven at 60 °C for 6 h to remove solvent. To remove the residual solvent, the white membrane (denoted as NTO CPE, thickness: 80 ~ 100 μm) was further put into a vacuum oven and dried at 100 °C for 12 h.

The same method was used to synthesize PVDF-HFP/$NaPF_6$ polymer electrolyte without NTO (denoted as blank SSE).

S1.5 Preparation of electrode and Assembly of battery

Coin cells (2032-type) were assembled in a high purity Ar-filled glove box with water and oxygen content lower than 0.1 ppm, and the solid-state electrolyte membrane (NTO CPE or blank SSE) was punched into a 12 mm diameter disc. The solid-state overall battery is composed of sodium metal anode, $Na_3V_2(PO_4)_3$ cathode and the as-prepared electrolyte membrane (NTO CPE or blank SSE). The $Na_3V_2(PO_4)_3$ (NVP) cathode is composed of the active material of $Na_3V_2(PO_4)_3$, the conductive agent of acetylene black, and the binder of polyvinylidene fluoride (PVDF) with a mass ratio of 7: 2: 1. The mixture was ground well and then dispersed in NMP, then the obtained slurry was spread on aluminum foil using a doctor blade. After dried in oven at 60 °C overnight and further in vacuum oven at 100 °C for 12 h. The active material loading of the cathode is ~ 2.0 mg cm^{-2}. 10 μL of liquid electrolyte (LE, 1 M $NaPF_6$ in diglyme, DoDoChem Co) was dropped on the dried cathode during the assembly of the full battery to wet the interface for electrochemical test.

Sodium metal battery with commercial separator (Grade GF/D, Whatman Co.) and $NaPF_6$ electrolyte (1 M in diglyme) were also assembled for comparison.

Na|NTO|Na and Na|NTO CPE|Na symmetrical cells were also assembled to investigate the Na stripping/plating behavior in the presence of solid-state electrolyte of NTO or NTO CPE.

In order to explore the Na^+ storage behavior of NTO, Na|LE|NTO cell was assembled with liquid electrolyte (LE) of $NaPF_6$ (1 M in diglyme) and commercial separator (Grade GF/D), in which sodium metal, the recrystallized NTO as anode and cathode, respectively. The fabrication of the NTO cathode was as same as that of the $Na_3V_2(PO_4)_3$ cathode except that the recrystallized NTO was utilized as the active material instead of $Na_3V_2(PO_4)_3$.

S1.6 Battery test

The LAND CT-2001A system was used to charge and discharge the assembled cells at room temperature. The rate performances of Na|NTO CPE|$Na_3V_2(PO_4)_3$ (NVP) Na|blank SSE|NVP and Na|LE|NVP full batteries were measured in the potential range of 2.5 ~ 3.8 V *vs.* Na^+/Na. The current densities are stepwise from 0.02, 0.05, 0.08, 0.1, 0.2 to 0.5 A g^{-1} and then back to 0.02 A g^{-1} with five cycles at each current density. In order to detect the redox plateau of NTO, in the rate capability test of Na|LE|NTO cell, the voltage window was set as 0.5 ~ 3.8 V. The cycling performances of the above full batteries were all measured in the potential range of 2.5 ~ 3.8 V *vs.* Na^+/Na at 0.1 A g^{-1}.

The electrochemical impedance spectra (EIS) of Na|NTO CPE|$Na_3V_2(PO_4)_3$ (NVP) and Na|blank SSE|NVP cells were measured with an amplitude voltage of 5 mV in the frequency range of 0.01 Hz ~ 10^6 Hz using an electrochemical workstation (CHI660e, Shanghai Chenhua, China). Before the EIS measurement, the cells were tested at 100% SOC, and was left standing for 20 min.

Sodium stripping/plating behavior was characterized through galvanostatic experiment under 2.0 mA cm^{-2} on Na|NTO|Na or Na|NTO CPE|Na symmetric cell until the capacity reach 2.0 mAh cm^{-2}, then the process was carried out repeatedly. And critical current density (CCD) test was under a lifting current density from 0.2 to 4.0 mA cm^{-2}.

S1.7 Electrochemical measurement

The ionic conductivity (σ, S cm^{-1}) of the as-prepared SSE (NTO or NTO CPE) was measured by EIS (CHI660e) of stainless steel (SS)|NTO|SS or SS|NTO CPE|SS blocking cell with an AC amplitude of 10 mV in the frequency from 10^6 to 0.01 Hz. The test was conducted in the temperature from 25 to 65 °C to estimate activation energy. The ionic conductivity and activation energy were calculated using the following equation:

$$\sigma = \frac{L}{RS} \quad (1)$$

$$\sigma T = A \exp(\frac{-E_a}{K_B T}) \quad (2)$$

Where R (Ω) is the resistant value of solid-state electrolyte (NTO or NTO CPE) obtained by EIS, L (cm) and S (cm^2) are the thickness and area of solid-state electrolyte, respectively. E_a (eV) is ion transport activation energy; A is pre-exponential factor; T is absolute Temperature (K); and K_b is Boltzmann constant (1.381×10^{-23} J K^{-1}).

Electrochemical windows of NTO and NTO CPE were tested by liner sweep scanning (LSV) from 2 to 6 V on Na|NTO|SS and Na|NTO CPE|SS cells.

The Na^+ transfer number (t_{Na+}) was obtained through potentiostatic experiment, in which 10 mV of step potential was applied on Na|NTO|Na or Na|NTO CPE|Na symmetrical cells for 2000 s to obtain initial and steady currents for calculation. The calculation equation is as follow:

$$t_{Na^+} = \frac{I_s (\Delta V - I_0 R_0)}{I_0 (\Delta V - I_s R_s)} \quad (3)$$

Where ΔV is the applied voltage (10 mV), I_0 and I_S are the initial and steady current through the cell measured on CHI 660E workstation. R_0 and R_s are the initial and steady resistances collected by EIS.

S1.8 Material characterization

Crystal structure information of sample was acquired by powder X-ray diffractometer (PANalytical X'pert Pro MPD) with Cu Kα radiation (λ= 1.54056 Å). And Rietveld refinement was performed using the TOPAS 5.0 software package (Bruker). The metallic (Na and Ti) elemental contents were determined by inductively coupled plasma optical emission spectroscopy (ICP-OES 6300 Duo, Thermo). The electrical conductivity of NTO was measured by a four-contact probe system with a high precision resistivity meter (FM100GH, Xi'an Honghu Instrument Co., Ltd) at room temperature in ambient atmosphere. Thermogravimetric (TG) analysis was conducted on a METTLER TOLEDO TGA2 analyzer in N_2 atmosphere with a heating rate of 10 °C min^{-1} from room temperature to 800 °C. Raman spectroscopy was performed on Labram HR Evolution Raman spectrometer. X-ray photoelectron spectroscopy (XPS) analysis was tested by a ESCALAB 250 analyzer. Electron paramagnetic resonance (EPR) spectroscopy analyses was performed using

an EPR (BRUKE EMXPLUS) with the center field of 3510 G and sweep width of 100 G. Scanning electron microscopy (SEM) and energy-dispersive spectroscopy (EDS) as well as elemental mappings were recorded by Thermo Fisher (Quattro S) instrument equipped with EDS (AMETEK) analyzer. Transmission electron microscopy (TEM), high resolution TEM (HRTEM) and selected area electron diffraction (SAED) patterns were obtained by using a Thermo Fisher Talos F200s apparatus along with an EDS spectroscope (Super-X). High-angle annular dark-field (HAADF)-scanning transmission election microscope (STEM) pattern was performed at a Talos 200S TEM equipped with dual-detector super EDS system, and EDS mappings were acquired at 200 kV with a convergence semi-angle of 22.5 milliradian. The dwelling time was 2 μs per pixel, and the collection angle was 46-200 milliradian. Infrared Spectroscopy (IR) measurements were collected by using IR spectrometer (IRTracer-100) with wavenumber range from 400 to 4000 cm^{-1}.

S1.9 Computational details

Nudged elastic band Calculation (NEB) [2] was performed by utilizing the Vienna ab initio simulation package (VASP) code [3, 4] for Na^+ migration along the *ac* plane. A Na^+ ion was removed from the original structure to create a vacancy for Na^+ migration. Static relaxation was done for initial and final structures, the energy convergence criterion was set to 10^{-6} eV and a force convergence criterion was set to 0.02 eV $Å^{-1}$. And then five images were linearly interpolated between the initial and final structure for NEB calculation. The energy convergence criterion in NEB calculation was adjusted to 10^{-6} eV and the force convergence criterion was set to 0.01 eV $Å^{-1}$. The energy barrier ΔE was calculated by the difference between the maximum and initial energies along the entire migration pathway.

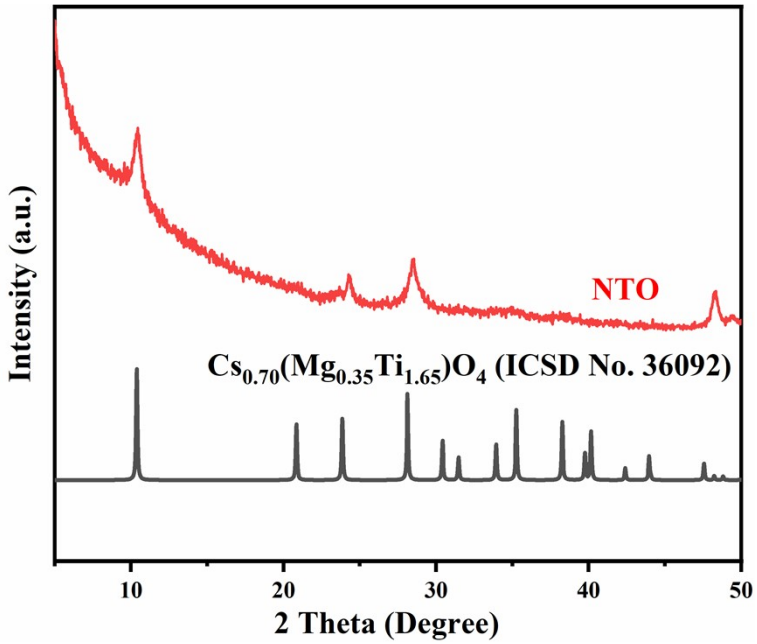

Fig. S1 XRD pattern of NTO and the simulated profile of $Cs_{0.70}(Mg_{0.35}Ti_{1.65})O_4$ (ICSD No. 36092).

S2 TG analysis and Raman spectrum of hydrate NTO

The TG curve of hydrated NTO was measured at a heating rate of 10 °C min^{-1} in a N_2 atmosphere (**Fig. S2a**). The weight loss (~5.8 %) from room temperature to 100 °C corresponds to the adsorbed water on the surface, indicating that the sample exhibits good affinity towards water molecules. The weight loss (~5.8 %) in the range of 100 ~ 200 °C is probably associated with the crystal water, which is approximately equal to 0.5 molar water molecule per formula unit, suggesting the stoichiometric molecular formula of $Na_{0.96}Ti_{1.26}O_3 \cdot 0.5H_2O$.

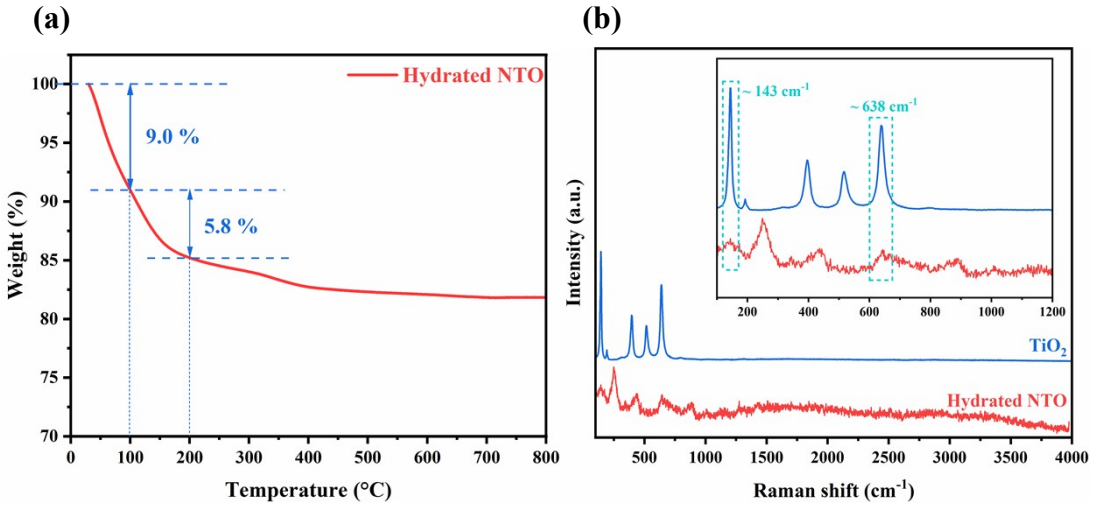

Fig. S2 (**a**) TG curve of hydrated NTO; (**b**) Raman spectra of hydrated NTO and commercial TiO_2.

As shown in **Fig. S3**, hydrated NTO and commercial TiO_2 exhibit similar Raman peaks at ~ 143 and ~ 638 cm^{-1}, which is due to the presence of Ti-O-Ti linkage in their frameworks.[5] In addition, it is found that the Raman peaks in the range of 200 ~ 1200 cm^{-1} of hydrated NTO are completely different from those of commercial TiO_2, which is due to the insertion of Na^+ between the Ti-O-Ti layers, resulting in significant changes in the coordination mode of Ti and the Ti-O bond lengths.

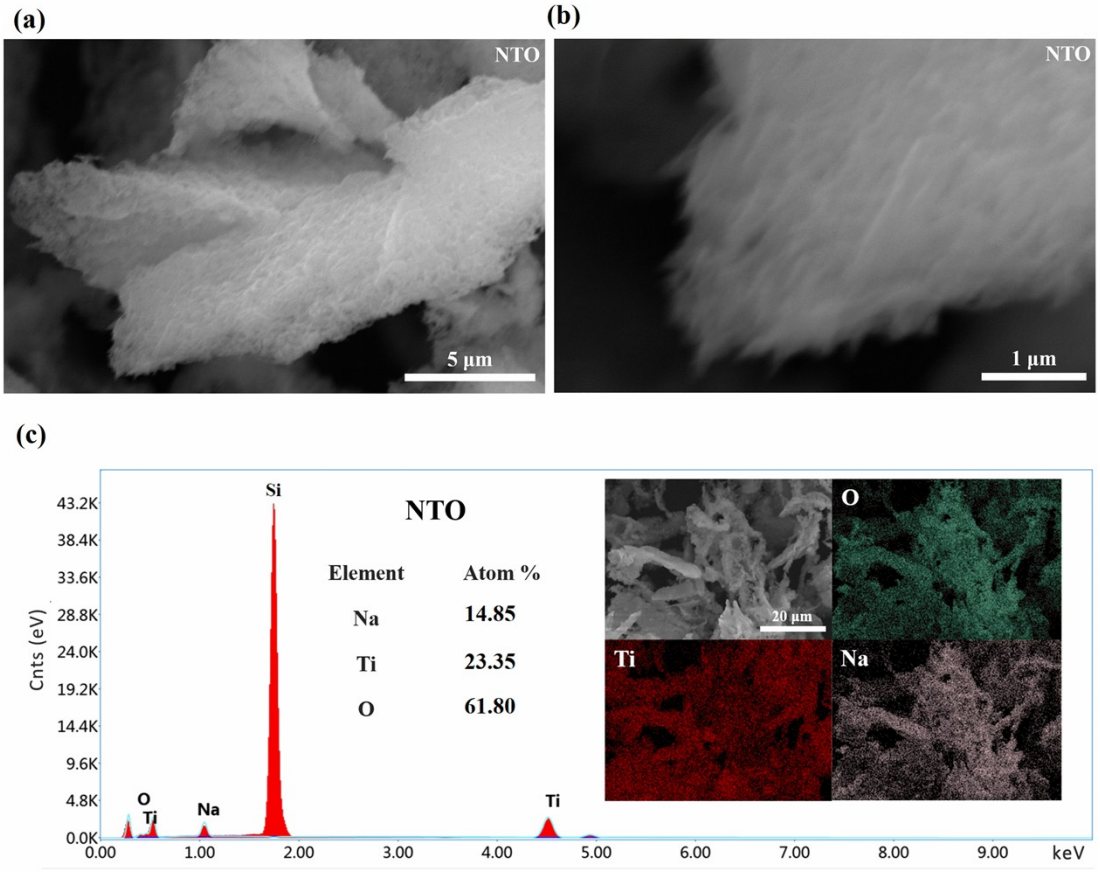

Fig. S3 (**a, b**) SEM and (**c**) EDS as well as elemental mappings of NTO.

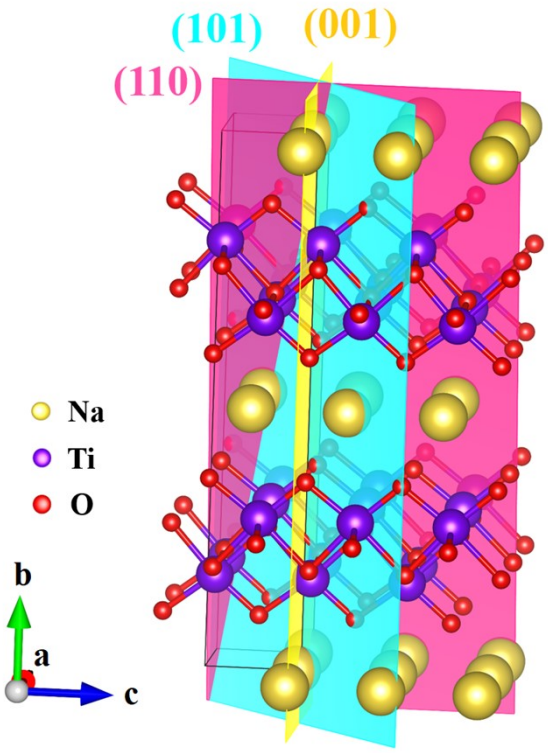

Fig. S4 The relative position of the (001), (110) and (101) facets as well as the interlayer channel along the *ac*-plane (the *ac*-diagonal ([101]) direction) in NTO.

S3 SAED patterns of NTO microneedle and microsheet

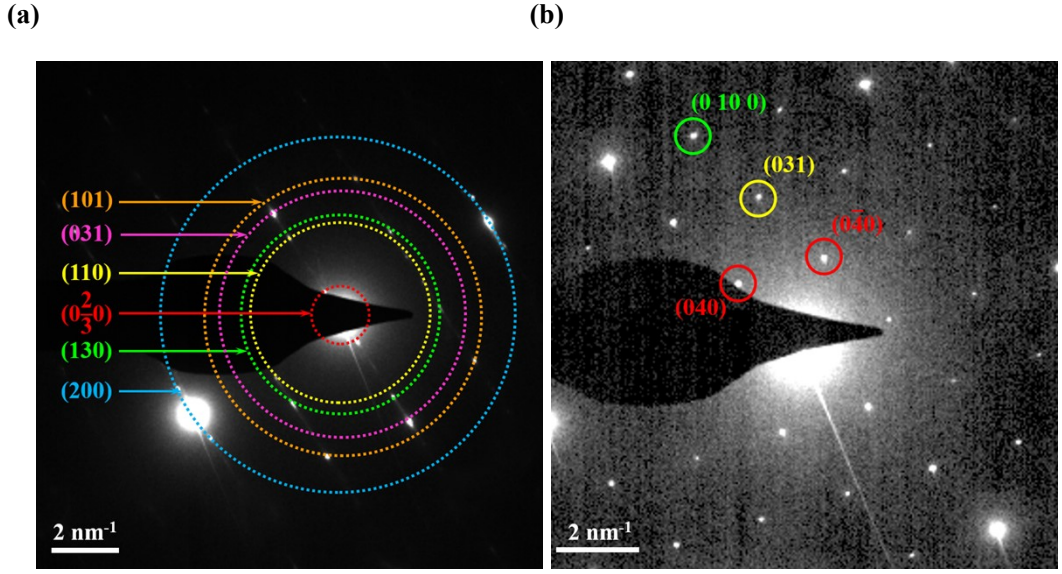

Fig. S5 SAED patterns of (**a**) NTO microneedle and (**b**) microsheet.

As shown in **Fig. S5a**, the SAED pattern of the NTO microneedle shows polycrystalline diffraction points with *d* spacings of 11.3, 3.7, 3.2, 2.7, 2.4 and 1.9 Å,

corresponding to the (0 2/3 0), (110), (130), (031), (101) and (200) crystal planes, which is in good agreement with the XRD and HRTEM results. And in the SAED pattern of the NTO microsheet, the diffraction spots of the (031) and (040) facets are also clearly observed (**Fig. S5b**), which is consistent with its HRTEM image.

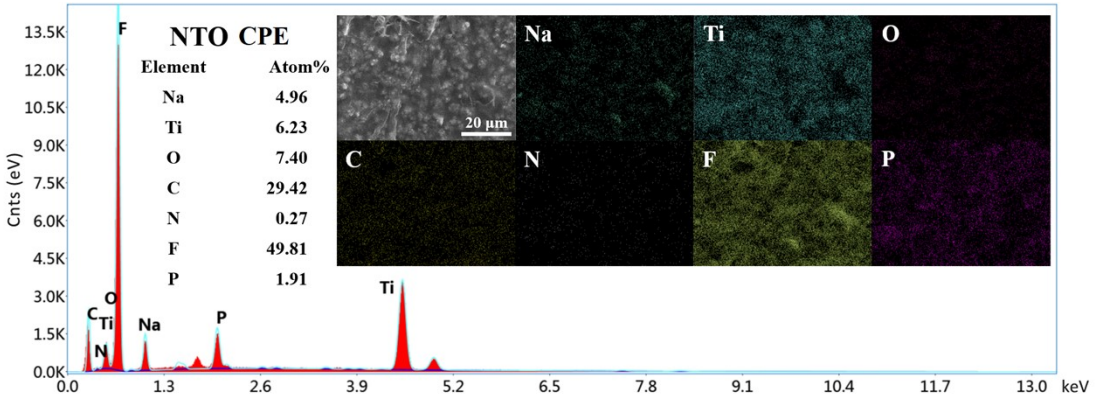

Fig. S6 EDS and elemental mappings of NTO CPE.

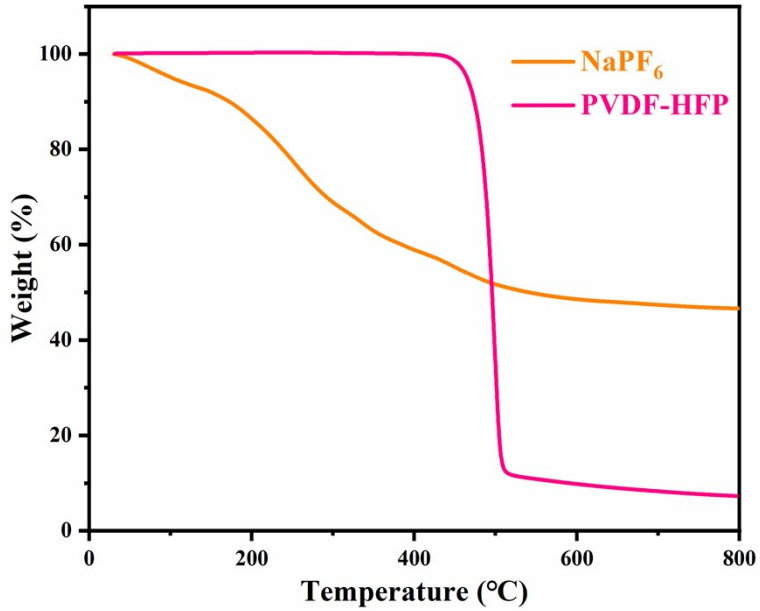

Fig. S7 TG curves of PVDF-HFP and $NaPF_6$.

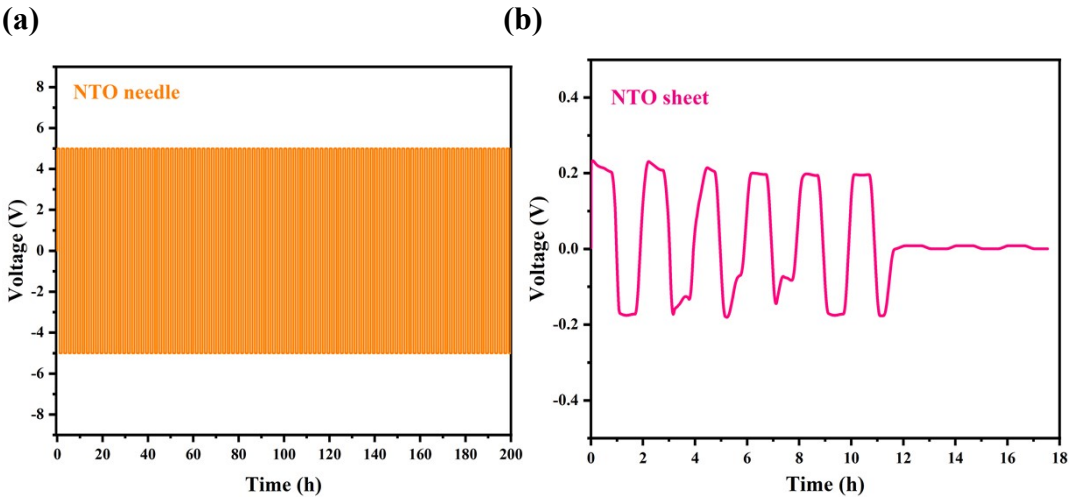

Fig. S8 (**a**) Voltage responses of (**a**) Na|NTO needles |Na and (**b**) Na|NTO sheets |Na symmetric cells at 0.2 mA cm^{-2}. (The maximum and minimum voltages of the instrument are set as +5 and -5 V).

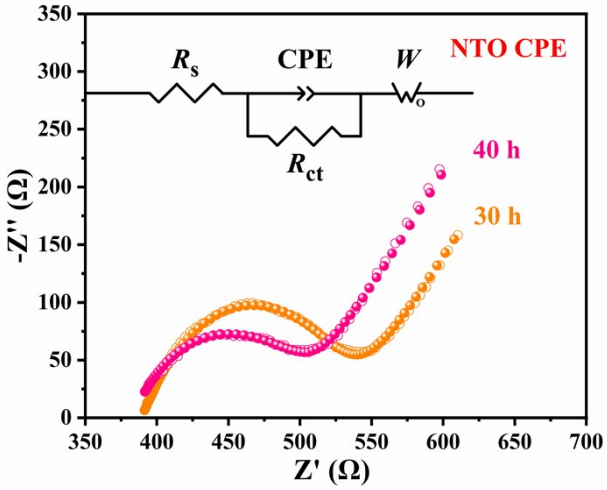

Fig. S9 Nyquist plots of the NTO CPE over 30 h- and 40 h-cycling test of the Na| NTO CPE |Na symmetric cell at 2.0 mA cm^{-2}.

.

S4 The redox property of NTO

In order to investigate the redox behavior of NTO, NTO was utilized as cathode for the fabrication the Na | LE | NTO cell to explore the redox activity of NTO. As shown in **Fig. S10(a, b)**, at lower current density of 0.02 A g^{-1}, the initial discharge specific capacity of the NTO cathode in the potential range of 0.5 ~ 3.8 *vs*. Na^+/Na can reach ~

147 mAh g^{-1} though the redox response of NTO mainly focuses on the low voltage range (< 1.0 V). In addition, in the potential range of 2.5 ~ 3.8 *vs*. Na^+/Na, the capacity retention of NTO at 0.1 A g^{-1} is ~ 90 %, illustrating an outstanding structural stability of NTO (**Fig. S10c**).

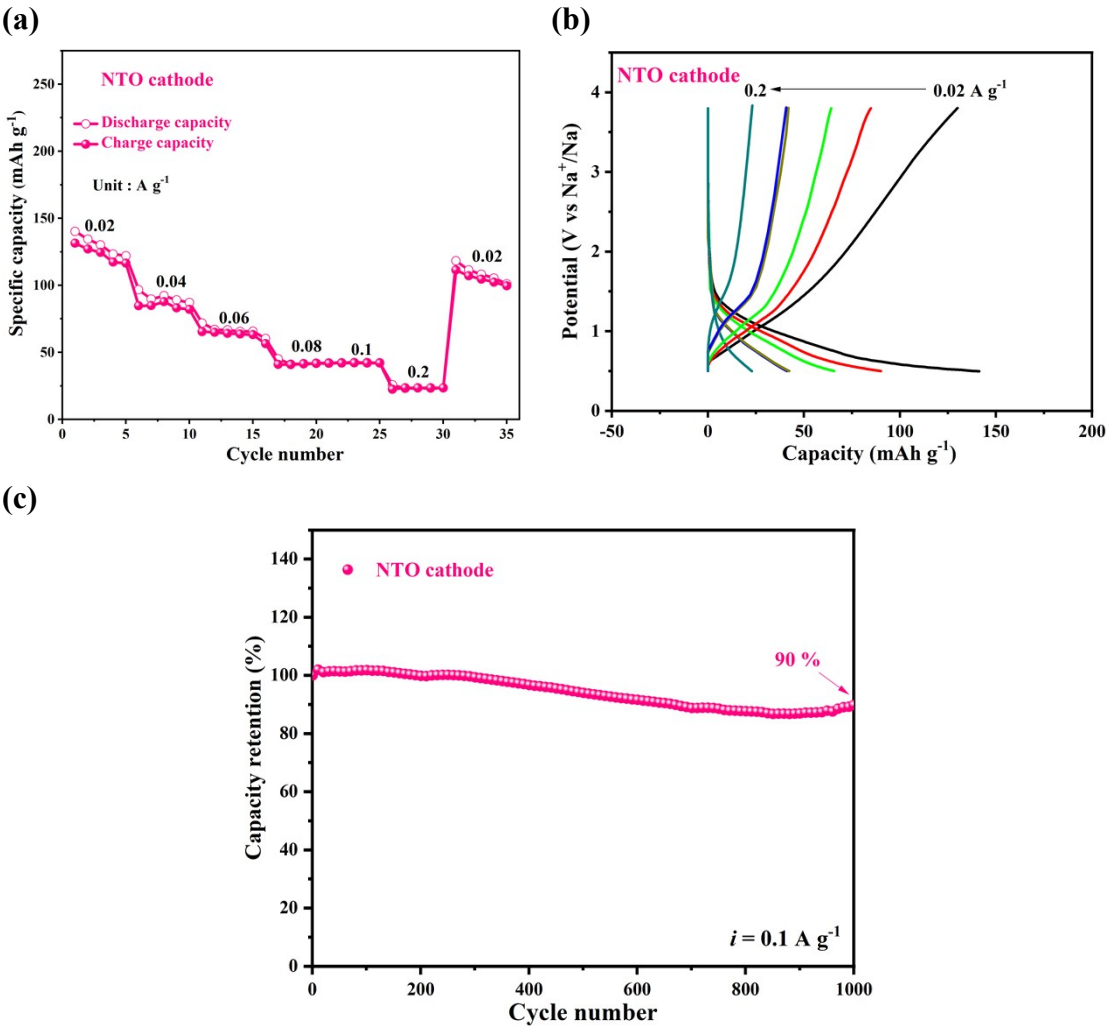

Fig. S10 (**a**) The rate capability of NTO in the potential range of 0.5 ~ 3.8 *vs*. Na^+/Na and (**b**) the corresponding charge-discharge profiles; (**c**) Cycling performance of NTO in the range of 2.5~ 3.8 *vs*. Na^+/Na at 0.1 A g^{-1}.

S5 The rate capability and cycling performance *of* Na | blank SSE | NVP full battery

As shown in **Fig. 6c**, in the presence of blank SSE without NTO, the cell can only operate normally at lower current densities (no more than 0.1 A g^{-1}), and the discharge specific capacities are significantly lower than those in the presence of NTO CPE or

LE. When the current density exceeds 0.1 A g^{-1}, a short circuit occurs. Similar short-circuit phenomenon is also observed in the early stage (~ 35 cycles) of the cycling test (**Fig. 6e**). It is associated with the aggregated grains in the blank membrane and inhomogeneous morphology of the blank SSE (**Fig. 4c, d**), which can not offer an even Na^+ transfer pathway.

(a)

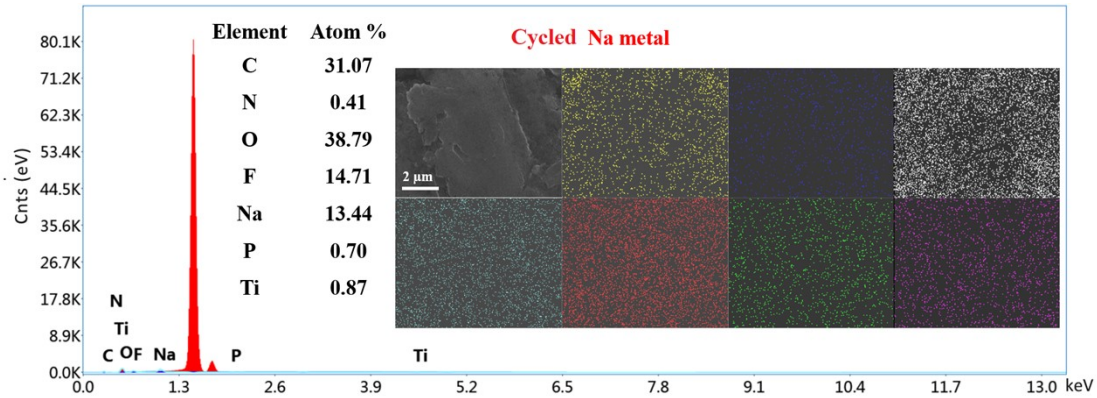

(b)

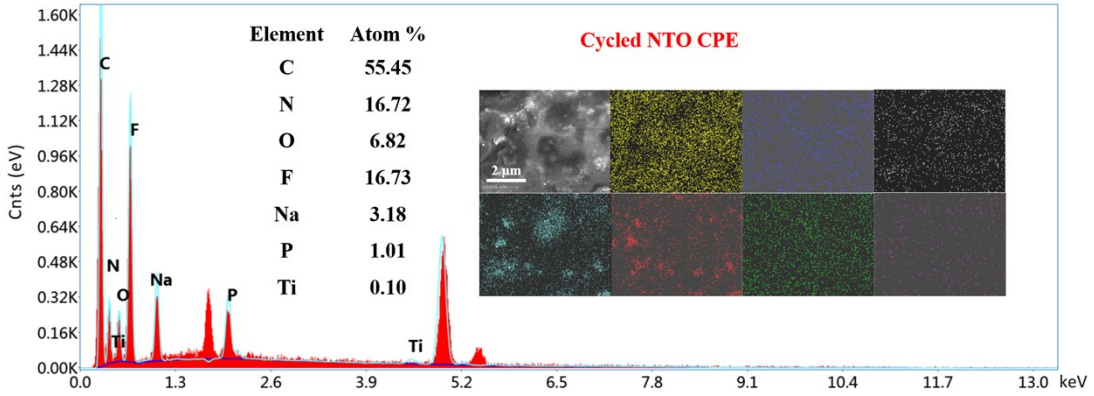

Fig. S11 EDS as well as elemental mappings of (**a**) the Na metal and (**b**) NTO CPE surfaces from the cycled Na| NTO CPE |Na symmetric cell.

Reference:

1. W. Han, H. S. Lee, B. Yoo and H. H. Park, *J. Alloys Compd.*, 2017, **695**, 2160-2164.
2. G. Henkelman and H. Jonsson, *Journal Of Chemical Physics*, 2000, **113**, 9978-9985.
3. G. Kresse, *Journal Of Non-Crystalline Solids*, 1995, **193**, 222-229.
4. G. G. Kresse and J. J. Furthmüller, *Phys. Rev. B, Condensed matter*, 1996, **54**,

11169.
5. Y. Cao, Q. Ye, F. Wang, X. Fan, L. Hu, F. Wang, T. Zhai and H. Li, *Adv. Funct. Mater.*, 2020, **30**, 2003733.